



Universiteit
Leiden
The Netherlands

Quantum computation with Majorana zero modes in superconducting circuits

Heck, B. van

Citation

Heck, B. van. (2015, May 6). *Quantum computation with Majorana zero modes in superconducting circuits*. *Casimir PhD Series*. Retrieved from <https://hdl.handle.net/1887/32939>

Version: Not Applicable (or Unknown)

License: [Leiden University Non-exclusive license](#)

Downloaded from: <https://hdl.handle.net/1887/32939>

Note: To cite this publication please use the final published version (if applicable).

Cover Page



Universiteit Leiden



The handle <http://hdl.handle.net/1887/32939> holds various files of this Leiden University dissertation.

Author: Heck, Bernard van

Title: Quantum computation with Majorana modes in superconducting circuits

Issue Date: 2015-05-06

Chapter 1

Introduction

When we solve the Schrödinger equation to study the evolution of a quantum system, the solution takes the form of a vector $|\Psi(t)\rangle$ in the Hilbert space. Unlike the more familiar Euclidean space of classical mechanics, it is hard to gain intuition about the Hilbert space using our everyday experience of the physical world. Indeed, $|\Psi(t)\rangle$ is usually a very large vector with complex entries, making it difficult to visualize its trajectory. The vastness of the Hilbert space makes the solution of the Schrödinger equation computationally very expensive, to the point that a full solution for $|\Psi(t)\rangle$ is often out of reach. Rather than being discouraged, we may change point of view and take this fact as a great opportunity. That is, we can look at the quantum state as a computational resource, where information can be stored and manipulated by exploiting features of quantum mechanics such as superposition, entanglement and interference [1, 2]. Surprisingly, the computational power of quantum mechanics seems to supersede that of classical physics, making quantum information a promising field for technological innovation.

However, preparing and controlling at will a quantum state is not an easy task. First, we need to be able to reliably store a quantum state, protecting it from the decoherence due to interaction with the environment. Second, we need a quantum state to follow precisely the trajectory in the Hilbert space corresponding to a desired algorithm. In principle, both goals can be achieved using quantum error correction [3, 4], at the cost of an overhead in memory and time requirements. An alternative approach, *topological quantum computation* [5, 6], shows that it is possible to imagine quantum systems which are naturally endowed with a resilience to decoherence and the possibility to execute algorithms with great accuracy. The topological approach uses the fact that some two-dimensional condensed matter systems can host a class of identical particles – called *non-Abelian anyons* – whose exchange causes a measurable change in the quantum state of the system. An entire algorithm can then be realized as a longer sequence of exchanges involving many particles. The algorithm does not rely on the details of how the exchanges are performed – similar trajectories will yield identical results – and is thus topological in nature. The quantum information

is encoded in the quantum state of the identical particles, and in the presence of an energy gap it stays protected as long as the particles stay far away from each other, or do not accidentally exchange their positions.

The theory of non-Abelian anyons is rooted in the abstract domains of mathematical physics and conformal field theory [7–10]. In condensed matter, non-Abelian anyons appeared first in the theory of the fractional quantum Hall effect [11–13] and later in that of superconductivity [14]. At present, there has been no clear experimental detection of non-Abelian statistics. The central theme of this thesis is to translate this set of beautiful ideas rooted in mathematical physics into a set of concrete devices where non-Abelian statistics can be demonstrated and used for quantum information purposes. The focus will be on the simplest type of particle which is known to obey non-Abelian statistics: Majorana modes occurring as zero-energy excitations in superconducting systems. We will see how the necessary manipulations of Majorana modes can be achieved using simple circuit elements such as capacitors and Josephson junctions, and thus arrive at a new concrete design for the experimental implementation of a fault-tolerant quantum computer. The two design principles behind this proposal are the use of Coulomb interaction as the fundamental physical mechanism permitting control of Majorana modes, and the use of magnetic fluxes as experimental knobs to tune these interactions.

In this introductory chapter, we introduce the main concepts necessary to follow the rest of the thesis. We first review the concept of identical particles in quantum mechanics by making use of the notion of the Berry phase. Then, we derive the non-Abelian statistics of Majorana modes and use them as a concrete example to understand how topological quantum computation works. Finally, we move on to describe how Majorana modes affect the behavior of superconducting circuits, and illustrate the fundamental design principles of our proposal for a *Coulomb-assisted, flux controlled* topological quantum computation with Majorana modes.

1.1 Identical particles and Berry's phase

The symmetrization postulate is one of the cornerstones of quantum mechanics [15]. It divides particles into bosons and fermions according to their spin, integer or half-integer respectively, and states that quantum states of bosons or fermions have to be symmetric or antisymmetric with respect to the permutation of the positions of any two particles in the system. The symmetrization postulate is supported by a large amount of experimental evidence: the periodic table of chemical elements, the electron Fermi sea in solids and the phenomenon of Bose-Einstein condensation are among its most direct consequences. Furthermore, it follows directly from the union of quantum mechanics with special relativity, which yields a connection between spin and statistics (in fact, the necessary ingredient for such a connection is the existence of anti-particles [16]).

Nevertheless, and most interestingly, the symmetrization postulate is not the end of the story [17]. In two spatial dimensions, quantum mechanics is compatible with

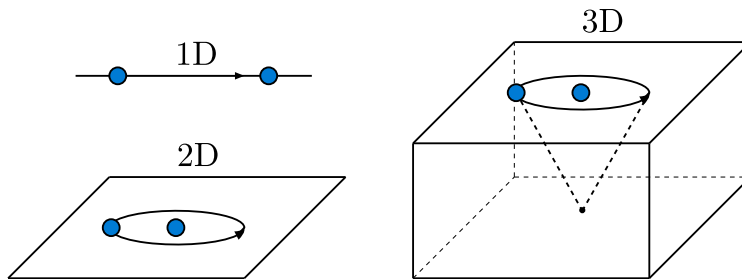


Figure 1.1: Exchanging identical particles in different dimensions. *Top left.* In one dimension, an attempt at exchanging two particles leads unavoidably to a collision. Hence, quantum statistics of identical particles can not be unambiguously defined. *Right.* In three dimensions (or more), the trajectory of a particle enclosing a second one can always be contracted to a single point. This fact implies that the exchange phase of the particles is constrained to two possible values only, corresponding to bosonic and fermionic statistics. *Bottom left.* In two dimensions, a loop around a particle cannot be contracted to a single point. Identical particles can therefore exhibit exotic quantum statistics.

the existence of particles, known as *anyons*, which do not obey bosonic or fermionic statistics. In order to see why two dimensions are special, we can consider the closed trajectory C of a particle around a second, identical particle (Fig. 1.1). This trajectory is equivalent to a sequence of two position exchanges between the particles, hence it gives direct insight into their exchange statistics.

The evolution of the system along the loop C is described by a unitary operator \mathcal{U} connecting the initial and final quantum states,

$$|\Psi(T)\rangle = \mathcal{U}(C, T) |\Psi(0)\rangle. \quad (1.1)$$

Here, T is time it takes the first particle to complete its trajectory. We consider a situation in which no “quantum jumps” occur: at all times $0 \leq t \leq T$, the quantum state $|\Psi(t)\rangle$ is an instantaneous eigenstate of the Hamiltonian with energy $E(t)$. Under these conditions, the quantum adiabatic theorem [15] states that as $T \rightarrow \infty$,

$$\mathcal{U}(C, T) = \exp \left[-i \int_0^T E(t) dt \right] \exp [i\gamma(C)]. \quad (1.2)$$

The first phase factor is the usual dynamical phase factor found in the solution of the Schrödinger equation. We are more interested in the second phase factor $\gamma(C)$, which is known as the Berry phase [18, 19],

$$\gamma(C) = \int_0^T \left\langle \Psi(t) \left| \frac{d\Psi(t)}{dt} \right. \right\rangle dt. \quad (1.3)$$

Since dt appears both on numerator and denominator in the expression above, the Berry phase does not depend on T nor on the kinematics of the trajectory, but only

on the loop C . In general, the Berry phase is the sum of two components. The first component depends on the *geometrical properties* of C – for instance, if an external magnetic field is present, this geometric contribution is the Aharonov-Bohm phase, which is proportional to the magnetic flux enclosed by the loop, and hence to the area of the loop. The second component only depends on the *topological properties* of C , i.e. on the winding number n , the number of times that the first particle encircles the second ($n = 1$ for the paths in Fig. 1.1). Different trajectories which can be continuously deformed into each other have the same winding number, and hence are characterized by the same topological contribution to the Berry phase. Its value is given by $2n\theta$, where θ specifies the quantum statistics of the two particles and the factor of two is due to the fact that every loop is equivalent to two exchanges.

As shown in Fig. 1.1, in three dimensions a closed loop C can always be deformed to a single point, that is to a trajectory where the first particle does not move at all. Therefore, the topological contribution to the Berry phase vanishes for all loops. We must in other words require that $2\theta = 0 \pmod{2\pi}$, which yields two possible exchange phases $\theta = 0$ or $\theta = \pi$, corresponding to bosonic and fermionic quantum statistics respectively. In two dimensions, however, the winding number of a loop can not be changed via a continuous deformation of the loop. Hence, in principle there is no restriction on the value of θ . Particles which have a value of θ different from 0 or π are called *Abelian anyons*.

So far we have implicitly assumed the state $|\Psi(t)\rangle$ to be non-degenerate. Let us now consider the case of a degeneracy D . In this case, the quantum state is specified by D components $|\Psi_n(t)\rangle$, and the Berry phase factor $\exp[i\gamma(C)]$ appearing in Eq. (1.2) has to be substituted by a $D \times D$ matrix [20],

$$U(C) = P \exp \left[\int_0^T A(t) dt \right]. \quad (1.4)$$

Here, P is the path-ordering operator and A is a skew-Hermitian matrix ($A^T = -A^*$) known as the Berry connection, with matrix elements $A_{nm}(t) = \langle \Psi_m(t) | d\Psi_n(t) / dt \rangle$. Like its one-dimensional counterpart, the Berry matrix $U(C)$ will have a geometric component and a topological one. It is therefore possible that the exchange of two particles results in a non-trivial unitary rotation in the degenerate ground state manifold. Crucially, Berry matrices corresponding to the exchange of two different pairs of particles need not commute. *Non-Abelian anyons* are precisely the class of identical particles having this property. In the following section, we will clarify this concept with a concrete and simple example which is central to the whole thesis: Majorana modes.

1.2 Non-Abelian statistics of Majorana modes

Majorana modes are mid-gap (zero energy) quasiparticles which can appear in superconducting systems with broken time-reversal and spin-rotation symmetry [22–24]. Since a clean superconductor does not allow for bulk excitations with energy smaller

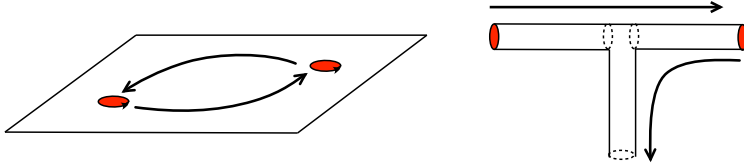


Figure 1.2: Majorana modes (red dots) can appear bound to vortices in superconducting thin films (left, [14]), or equivalently at domain walls in networks of quantum wires (right, [21]). In both cases, their positions can be exchanged in space, as depicted by the arrows. Because of the non-Abelian statistics of the Majorana modes, the procedure results in a non-trivial rotation on the quantum state of the superconductor.

than the pairing gap, a Majorana mode can be found either bound to a vortex in a superconducting film [14, 25] or localized at the end of a superconducting nanowire [26]. In virtue of particle-hole symmetry of the superconductor and in the absence of degeneracies, the creation and annihilation operators of a zero energy mode coincide: $\gamma = \gamma^\dagger$. Operators corresponding to different modes anti-commute, as normal fermionic operators, leading to the unusual set of relations

$$\gamma_n \gamma_m + \gamma_m \gamma_n = 2\delta_{nm}. \quad (1.5)$$

Note in particular that $\gamma_n^2 = 1$, so that we cannot speak of the Majorana mode being ‘empty’ or ‘occupied’. Out of two Majorana modes, say γ_1 and γ_2 , we can however construct an ordinary fermionic annihilation operator $c = \frac{1}{2}(\gamma_1 + i\gamma_2)$ satisfying $cc^\dagger + c^\dagger c = 1$. Hence, the two Majorana modes can be thought as the real and imaginary part of a conventional fermion mode. Their peculiarity is that they are well separated in space. This argument reveals that Majorana modes can only occur in pairs: if the number of vortices is odd, an additional mode must lie somewhere along the boundary of the superconductor. It also reveals that the two Majorana modes form a two-level system, with the two states differing by the presence or absence of a fermion. As long as the Majorana modes are kept at a distance much longer than the coherence length, the two levels are degenerate in energy, so that it is not costly to remove or add a fermion to the system.

Let us now consider a two-dimensional superconductor with $2N$ vortices hosting Majorana modes $\gamma_1, \dots, \gamma_{2N}$. We can group the Majorana modes in pairs to form N fermionic creation operators c_1, \dots, c_N . These operators span a degenerate manifold with 2^N states $|p_1 \dots p_N\rangle$ labeled by the occupation numbers $p_n = 0, 1$ of the N fermionic modes. In an isolated superconductor fermion parity is a conserved quantity, so the manifold is divided in two subspaces containing all the states of even and odd parity. They are distinguished by the eigenvalue ± 1 of the fermion parity operator

$$\mathcal{P} = i^N \gamma_1 \dots \gamma_{2N}, \quad \mathcal{P}^2 = 1. \quad (1.6)$$

Within the even or odd subspace, which have dimension 2^{N-1} , superpositions of states are allowed.

Let us see what happens when two vortices are adiabatically exchanged in space [27]. We might of course do so by computing the Berry matrix using Eq. (1.4). However, there is a more direct way which allows to arrive at the result without much effort. It is convenient to adopt the Heisenberg picture, where the Majorana operators depend explicitly on time. In particular, the two Majorana modes bound to the vortices being moved are related to the Berry matrix by the equation

$$\gamma_{n,m}(T) = U_{nm} \gamma_{n,m}(0) U_{nm}^\dagger, \quad (1.7)$$

up to a phase factor. We have denoted the Berry matrix as U_{nm} since it is natural to assume that it will only depend on the Majorana modes γ_n, γ_m involved in the exchange. Furthermore, U_{nm} has to preserve fermion parity, $[U_{nm}, \mathcal{P}] = 0$. This means that it can only depend on the product $\gamma_n \gamma_m$. Finally, unitarity imposes that the Berry matrix is of the form $U_{nm} = \exp(\alpha \gamma_n \gamma_m)$, with α a real coefficient to be determined. Direct calculation yields

$$\gamma_n(T) = \cos(2\alpha) \gamma_n(0) - \sin(2\alpha) \gamma_m(0), \quad (1.8a)$$

$$\gamma_m(T) = \cos(2\alpha) \gamma_m(0) + \sin(2\alpha) \gamma_n(0). \quad (1.8b)$$

We want the two operators to be interchanged by U , leading to the choice $\alpha = \pm\pi/4$. The sign of α distinguishes clockwise and counterclockwise exchanges of the vortices, the precise assignment being arbitrary. The final result is therefore

$$U_{nm} = \exp\left(\frac{\pi}{4} \gamma_n \gamma_m\right). \quad (1.9)$$

We see that the Berry matrix resulting from the exchange is not simply an overall phase, but a non-trivial rotation in the ground state manifold. Also, we see that Berry matrices corresponding to exchanges of different pairs do not commute if the two pairs share one Majorana, and commute otherwise.

To understand the multiplication properties of these matrices better, let us imagine that initially all Majoranas are ordered on a line according to their index n . The exchange between any pair of Majoranas can be generated via a succession of exchanges between neighboring Majoranas, hence we may focus on the matrices $U_{n,n+1}$. To keep track of all the exchanges, we may imagine that a strand is attached to each vortex, such that a succession of exchanges forms a braid out of the $2n$ strands. We see that to each different braid, we may associate a corresponding unitary operator via a multiplication of an appropriate sequence of matrices $U_{n,n+1}$. It can be checked that these matrices obey the following relations,

$$U_{n,n+1} U_{n+1,n+2} U_{n,n+1} = U_{n+1,n+2} U_{n,n+1} U_{n+1,n+2}. \quad (1.10)$$

Mathematically, these are precisely the relations obeyed by the generators of the *braid group*, which is a generalization of the permutation group to a situation where the order of the exchanges matter. For this reason, the exchange of two Majorana modes (or of non-Abelian anyons in general) is usually referred to as *braiding*.

1.3 Topological quantum computation

The discussion of the previous section is a good starting point to understand topological quantum computation more in detail, using Majorana modes as a practical example of non-Abelian anyons. The main ideas are the following:

1. The ground state manifold of $2N$ Majorana modes is taken as the computational space. At a fixed total fermion parity, it forms a register of $N - 1$ qubits. The physical degree of freedom which is used to encode the qubits is the fermion parity of pairs of Majorana modes, sometimes also referred to as their *topological charge*.
2. Operations on the register are performed by braiding Majorana modes in space.
3. Initialization and measurement of the register entries are carried out by bringing two Majorana modes very close to each other, an operation sometimes called *fusion*. When this happens, the ground state degeneracy splits, allowing for a readout of the fermion parity of the two joint Majorana modes.

It is essential that the ground state manifold is protected by an energy gap from the excited states. This ensures that the adiabatic limit can be reached when operating on the register, and protects the register from dissipation.

The advantages of this approach are:

1. The quantum gates which can be executed via braiding are extremely accurate and do not depend on the exact trajectory followed during the exchange. In this sense, they are extremely resilient to implementation inaccuracies.
2. The quantum state of the register is encoded in the fermion parity degrees of freedom, which are shared non-locally by the Majorana modes. This means that no local perturbation can change the state of the register and cause decoherence. An experimentally relevant exception is a change in fermion parity due to the tunneling of a stray quasiparticle into the system (quasiparticle poisoning).

A crucial question in topological quantum computation is whether braiding operations are universal, in the sense that any unitary operation on the register can be approximated with arbitrary accuracy by a finite sequence of braiding operations. Unfortunately, this is not the case for Majorana modes. In this case, braiding operations have to be supplemented by non-topological ones.

So far our discussion has not addressed the problem of how to initialize, braid and measure Majorana modes in practice. As already mentioned and as discussed in more detail in the next section, our proposal is to use microwave superconducting circuits for all these purposes.

1.4 Superconducting circuits with Majorana modes

In superconducting circuits, macroscopic physical observables such as currents and voltages exhibit quantum behavior. In fact, superconducting circuits are one of the most prominent platforms for quantum information processing [28–31]. In this section we will describe in simple terms how Majorana modes affect the physics of superconducting circuits. In order to do so, we start by describing the “hydrogen atom” of superconducting circuits - the Cooper pair box.

1.4.1 Cooper pair box in the transmon limit

A Cooper pair box consists of two superconductors connected by a capacitor and a Josephson junction, possibly split in two arms, see Fig. 1.3. Cooper pairs can flow between the two island by quantum tunneling across the Josephson junction. This motion results in fluctuations in the voltage $v(t)$ and current $i(t)$ between the two nodes of the circuit. The dynamics of the system can be described in terms of the integrals of current and voltages, which are the phase and charge difference across the junction,

$$\phi = \frac{2\pi}{\Phi_0} \int_{-\infty}^t v(t') dt', \quad N = \frac{1}{e} \int_{-\infty}^t i(t') dt'. \quad (1.11)$$

Here, $\Phi_0 = h/2e$ is the superconducting flux quantum. These two quantities are canonically conjugate variables, similarly to position and momentum of a particle,

$$[\phi, N] = 2i. \quad (1.12)$$

The factor of two in the commutation relations is due to the fact that electrons form Cooper pairs in the superconducting condensate, and hence charge is transferred in units of $2e$ across the junction. The Hamiltonian describing the Cooper pair box is

$$H = E_C N^2 + E_J (1 - \cos \phi), \quad (1.13)$$

with $E_C = e^2/2C$ the charging energy and E_J the Josephson energy. In the split-junction geometry, the Josephson energy can be varied by threading a magnetic flux Φ in the loop formed by the two arms of the junction. Neglecting any asymmetry between the strengths of the two arms, one has $E_J = E_{J,0} \cos(\pi\Phi/\Phi_0)$.

The circuit exhibits quantized energy levels, which are observable provided that temperature and damping-induced broadening of the levels are both much smaller than the level spacing. We will be particularly interested in the limit $E_J \gg E_C$, where the level spacing is approximately constant,

$$E_n \simeq \hbar\Omega(n + 1/2), \quad (1.14)$$

where $\hbar\Omega = \sqrt{8E_J E_C}$ is the plasma frequency, which characterizes current oscillations across the Josephson junction. Typical values of Ω are in the range 5 to 30 GHz,

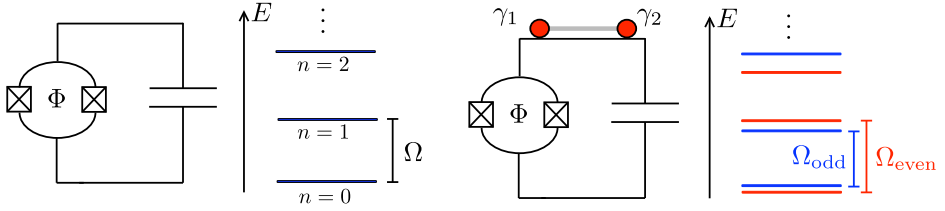


Figure 1.3: *Left*: A Cooper pair box with a split Josephson junction. When the Josephson energy is much larger than the charging energy, and at very low temperatures, the energy spectrum consists of almost equally spaced levels separated by the plasma frequency $\Omega \simeq \sqrt{8E_J E_C}$. *Right*: If one of the two islands hosts Majorana modes (red circles), for instance appearing at the ends of a nanowire (grey), every level splits into a doublet of levels with different fermion parity [35].

allowing the system to be controlled with microwave radiation, using all the technology of RF electronic engineering. A Cooper pair box in this regime and coupled to a transmission line resonator constitutes a *transmon*, one of the most common and successful superconducting qubits.

Importantly, the Cooper pair box Hamiltonian only describes the quantum dynamics of the superconducting condensate, neglecting the contribution of unpaired quasiparticles. In principle, this description is accurate when $k_B T \ll \Delta$, the superconducting gap. Only states of even fermion parity are then relevant to the dynamics of the circuit, as states with odd parity have all energies greater than Δ . In practice, however, non-equilibrium quasiparticles are often observed in superconducting circuits even at very low temperatures, and cause random switches in the fermion parity of a superconducting island. For the sake of conceptual simplicity, and also motivated by recent progress in the enhancement of the parity lifetime of superconducting circuits [32–34], in what follows we disregard this complication.

1.4.2 Flux-controlled Coulomb interaction of Majorana modes

If one of the two superconducting islands forming the Cooper pair box hosts two Majorana modes γ_1 and γ_2 , one quasiparticle can be accommodated with no energy cost. The situation changes drastically, because now there are now two distinct superconducting condensates, one with even and one with odd parity. In the limit $E_C \rightarrow 0$, when the phase ϕ becomes a good quantum number, the even and odd states are to a good approximation given by a coherent superposition of all the charge states with the appropriate parity,

$$|\phi, e\rangle = \sum_n e^{i\phi n} |2n\rangle, \quad (1.15a)$$

$$|\phi, o\rangle = \sum_n e^{i\phi(n+1/2)} |2n+1\rangle. \quad (1.15b)$$

Even and odd states behave differently with respect to a shift of the superconducting phase by 2π : $|\phi + 2\pi, e/o\rangle = \pm|\phi, e/o\rangle$. In other words, even and odd states are respectively periodic and anti-periodic under a shift of ϕ by 2π . This boundary condition imposes a constraint between the Majorana operators and the number operator [36],

$$i\gamma_1\gamma_2 = (-1)^N. \quad (1.16)$$

The expression above is the mathematical statement corresponding to the fact that the fermion parity of a superconductor with Majorana modes is equal to the total charge contained in the superconductor, modulo $2e$. Eq. (1.16) is a gauge constraint on the Hilbert space of the Cooper pair box with Majorana modes. It has to be taken into account when solving the Cooper pair box Hamiltonian (1.13). A way to do so is to make a unitary transformation $|\Psi\rangle \mapsto R|\Psi\rangle$, with

$$R = \exp[i(1 - i\gamma_1\gamma_2)\phi/4]. \quad (1.17)$$

This transformation acts trivially on the even states, but makes the odd states periodic under a shift of ϕ by 2π . The Hamiltonian becomes (recall that $N = -2i\partial_\phi$)

$$RHR^\dagger = E_C[N + (1 - i\gamma_1\gamma_2)/2]^2 + E_J(1 - \cos \phi). \quad (1.18)$$

We see that the Majorana modes now appear explicitly in the charging energy term. At the same time, since the new Hamiltonian acts on a space of 2π -periodic functions, the eigenvalues of N are restricted to the even numbers. Note that the argument would apply equally to the case of a superconductor having more than two Majorana modes - in this case, the product $i^N\gamma_1 \dots \gamma_{2N}$ would appear in the Hamiltonian instead of $i\gamma_1\gamma_2$.

One might at first be surprised that Majorana modes are related to the charge in the superconductor, since they are usually presented as neutral objects. The neutrality of the Majorana modes is due to the presence of a superconducting condensate, which ‘‘absorbs’’ the charge corresponding to the fermion parity encoded in a pair of Majorana modes. In a grounded superconductor it is possible to forget about the charge degrees of freedom by fixing the phase ϕ of the superconductor, so that the boundary condition becomes irrelevant. However, in a floating superconductor this is no longer possible, and the relation between fermion parity and electric charge has to be restored explicitly.

In the transmon limit, one finds that the energy spectrum of the Cooper pair box with Majorana modes is given by a sequence of closely spaced doublets corresponding to states with different parity. Subsequent doublets are still separated by the plasma frequency $\hbar\Omega$. The n -th doublet has a parity-dependent energy splitting given by

$$\Delta_n \simeq E_C \left(\frac{E_C}{2E_J} \right)^{n/2+3/4} \exp\left(-\sqrt{8E_J/E_C}\right). \quad (1.19)$$

The expert reader may recognize in the above expression the charge dispersion of a transmon [37]. In fact, the change in the energy spectrum due to the parity encoded in

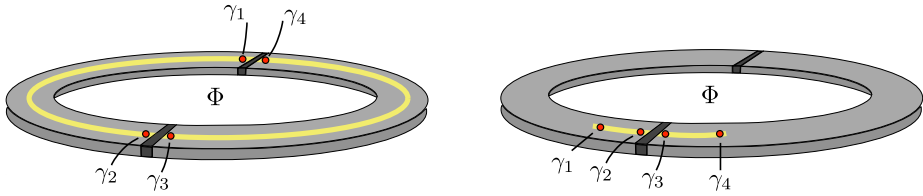


Figure 1.4: The two DC SQUID geometries studied in chapter 2, where we show that, in the presence of charging energy, the system shown in the left has a 4π -periodic Josephson energy, while the one on the right has a 2π Josephson-energy due to quantum phase slips through the Josephson junction without Majorana modes.

the Majorana mode is equivalent to the change determined by increasing or decreasing by e the induced charge on the capacitor plates.

Eq. (1.19) has two important consequences for our purposes. The first is that the frequencies of the circuit become parity-dependent, as also shown in the rightmost panel of Fig. 1.3. For the two lowest transmon states, the difference $\hbar(\Omega_{\text{even}} - \Omega_{\text{odd}})$ is typically in the range 1 to 100 MHz. Such a frequency shift in a transmon can be easily detected using microwaves, and the detection allows us to measure the fermion parity of the Majorana modes. The second consequence is that the parity splitting is very sensitive to the ratio E_J/E_C . This means that using a split junction and varying the flux Φ by half of a superconducting flux quantum, the energy splitting between different fermion parity states can be varied by a few orders of magnitude.

This exponential sensitivity gives us a very practical handle to operate on the quantum state of a collection of Majorana modes, while still keeping them at distances much larger than the coherence length. This is the main design principle behind our proposal for a superconducting implementation of topological computation.

1.5 This thesis

Before moving on, we give here an outline of the contents of this thesis. In chapters two to six, we will develop in detail the theory of Majorana modes in superconducting circuits and the blueprint for a topological quantum computer which is based on that theory. Chapter seven reports on the first experimental realization of hybrid superconducting microwave circuits with semiconducting nanowires¹. The remaining chapters extend the results of the first six chapters in different directions and physical systems. Chapter eight discusses how to measure and manipulate Majorana modes in fractional quantum Hall systems, while chapter nine generalizes the Majorana braiding scheme developed in chapter two to a generic model of non-Abelian anyons. Finally, chapter ten is a study of superconducting arrays in the presence of electron

¹The experiments described in chapter seven were performed in Dr. Leo DiCarlo's group in Delft. My contribution consisted in the theoretical analysis and interpretation of the experimental data.

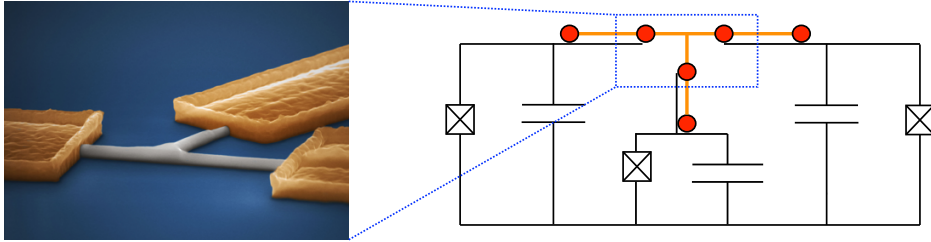


Figure 1.5: The superconducting circuit introduced in chapter three, able to perform flux-controlled braiding of Majorana modes. An essential element of the circuit is a T-junction, such as the InSb nanocross [38] shown in the image on the left (image courtesy of the Kouwenhoven group, TU Delft).

fractionalization, and chapter eleven a study of the transport properties of a linear array of superconducting islands with Majorana modes. We now give a brief description of the content of each chapter.

Chapter two. A peculiar signature of Majorana modes is the fact that the Josephson energy of two superconducting islands containing Majorana modes is a 4π -periodic function of the superconducting phase difference. If the islands have a small capacitance, their ground state energy is governed by the competition of Josephson and charging energies. In this chapter, we calculate this ground state energy in the ring geometries of Fig. 1.4. We show that the dependence on the Aharonov-Bohm phase $2e\Phi/\hbar$ remains 4π -periodic regardless of the ratio of charging and Josephson energies — provided that the entire ring is in a topologically nontrivial state. If part of the ring is topologically trivial, then the charging energy induces quantum phase slips that restore the usual 2π -periodicity. This chapter elucidates the consequences of the parity constraint, Eq. (1.16), on the properties of superconducting circuits, and it provides a preliminary understanding on how one can control the coupling of Majorana modes using Coulomb interactions.

Chapter three. We show how to braid Majorana modes in a network of superconducting nanowires by control over Coulomb interaction. The key idea behind flux-controlled braiding is to control independently the charging energy of the three arms of a T-junction using flux bias lines. Hence, the required circuit essentially consists of three copies of a Cooper pair box connected by a T-junction, see Fig. 1.5. T-junctions can be realized using InSb nanowires [38], making the proposed circuit experimentally feasible. Furthermore, as we see further in chapter 6, the flux-controlled braiding scheme can in fact be adapted to other systems which can support Majorana modes, such as quantum spin-Hall insulator/superconductor heterostructures. An advantage of this proposal is that the positions of the Majorana modes do not need to be changed, and local control gates do not need to be tuned during the braiding

operation.

Chapter four. Here we build on the results of the previous chapter, expanding the circuit of Fig. 1.5 to a larger one where the state of the Majoranas can be initialized and the result of a braiding operation can be measured. We identify the minimal circuit that can perform the initialization–braiding–measurement steps required to demonstrate non-Abelian statistics of Majorana modes. We then analyze the scalability of the circuit from a quantum information perspective. To this purpose, we introduce a quantum register, which we call a Random Access Majorana Memory, that can perform a joint parity measurement on Majoranas belonging to a selection of topological qubits. Such multi-qubit measurements allow for the efficient creation of highly entangled states and simplify quantum error correction protocols by avoiding the need for ancilla qubits.

Chapter five. A major obstacle towards the experimental demonstration of non-Abelian statistics in nanowire networks might be constituted by the presence of disorder in the nanowires. Strong disorder may indeed induce the presence of accidental Majorana modes at unwanted positions in the nanowire networks. In this chapter, we show that the Coulomb-assisted braiding protocol of the previous two chapters can be efficiently realized also in the presence of accidental modes. In particular, the errors occurring during the braiding cycle are small if the couplings of the computational Majorana modes to the accidental ones are much weaker than the maximum Coulomb coupling which is necessary during the braiding operation.

Chapter six. In this chapter, we construct a minimal circuit to rotate a qubit formed out of four Majorana modes at the edge of a two-dimensional quantum spin-Hall insulator. This circuit is smaller than the one required for a braiding operation, and might represent a good intermediate step towards braiding. Indeed, unlike braiding operations, generic rotations have no topological protection, but they do allow for a full characterization of the coherence times of the Majorana qubit. The rotation is controlled by variation of the flux through a pair of split Josephson junctions in a Cooper pair box, without any need to adjust gate voltages. The Rabi oscillations of the Majorana qubit can be monitored via oscillations in the resonance frequency of the microwave cavity that encloses the Cooper pair box.

Chapter seven. We present and analyze measurement on quantum microwave circuits with hybrid Josephson elements, comprised of semiconducting InAs nanowires contacted by the highly-disordered superconducting alloy NbTiN. Capacitively-shunted single elements behave as weakly anharmonic oscillators, or transmons, but with electrically tunable transition frequencies. Double-element circuits display similar transmon-like behavior at zero applied flux, while when biased at half the flux quantum they exhibit instead a strongly anharmonic spectrum, similar to that of a flux qubit. Theoretical analysis of the data explains this behavior via the formation of a double-well Josephson potential, due to the non-sinusoidal current-phase relation

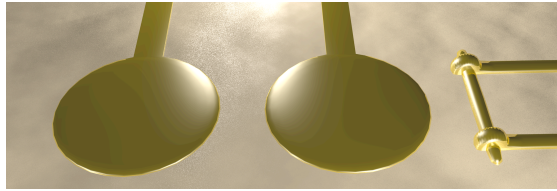


Figure 1.6: An illustration of the measurement device proposed in chapter 8 to measure the presence of the Majorana modes bound to charged quasiparticles in the $\nu = 5/2$ quantum Hall plateau. Two gates suspended on the quantum Hall liquid form two small dots, each binding a single quasiparticle. Double occupancy on one of the two dots comes with an extra energy cost associated with the fusion of two Majorana modes, and this energy can be detected by a charge sensor (right).

of the nanowire Josephson junctions. Close to half a flux quantum, we observe microwave-driven transitions between states with oppositely flowing persistent currents, manifesting macroscopic quantum coherence. The hybrid nanowire transmon devices presented in this chapter are magnetic-field compatible, hence they represent a first milestone on the road towards experiments combining superconducting circuits with Majorana modes.

Chapter eight. In this chapter, we shift our attention to the $\nu = 5/2$ quantum Hall plateau, whose fractionally charged quasiparticles are predicted to have an extra non-local degree of freedom, known as topological charge. This extra degree of freedom can in fact be understood as a Majorana mode bound to the quasiparticle. We show how this topological charge can block the tunneling of these quasiparticles, and how such *topological blockade* can be used to readout their topological charge (see Fig. 1.6), similarly to a charge readout of singlet-triplet qubits. We argue that the short time scale required for this measurement is favorable for the detection of the non-Abelian anyonic statistics of the quasiparticles. We also show how topological blockade can be used to measure braiding statistics, and to couple a topological qubit with a conventional one.

Chapter nine. The common approach to topological quantum computation is to implement quantum gates by adiabatically moving non-Abelian anyons around each other. However, chapters three and four of this thesis presented an alternative perspective based on the possibility of realizing the braiding of Majorana modes by adiabatically varying pairwise interactions between them, rather than their positions. In this chapter we show that this alternative approach is not specific to Majorana modes, but it works for generic non-Abelian anyons. We analyze a system composed by four anyons whose couplings define a T-junction and we show that the braiding operator of two of them can be obtained through a particular adiabatic cycle in the space of the coupling parameters. We also discuss how to couple this scheme with

anyonic chains in order to recover the topological protection.

Chapter ten. It is possible to generalize the notion of Majorana modes to system with electron fractionalization. So-called parafermionic modes with non-Abelian statistics may indeed exist at the interface between a superconductor and a ferromagnet along the edge of a fractional topological insulator. This chapter studies two-dimensional architectures of these non-Abelian anyons, whose interactions are generated by the charging and Josephson energies of the superconductors. We derive low-energy Hamiltonians for two different arrays of fractional topological insulators on the plane, revealing an interesting interplay between the real-space geometry of the system and its topological properties. On the one hand, in a geometry where the length of the FTI edges is independent on the system size, the array has a topologically ordered phase, giving rise to a qudit toric code Hamiltonian in perturbation theory. On the other hand, in a geometry where the length of the edges scales with system size, we find an exact duality to an Abelian lattice gauge theory and no topological order.

Chapter eleven. The last chapter is dedicated to the study of the transport properties of a linear array of superconducting islands with Majorana modes. In particular, we investigate the effect of quantum phase slips on the linear response of the array to an external voltage or temperature gradient. The effective low-energy description of the wire is that of a Majorana chain minimally coupled to a dynamical \mathbb{Z}_2 gauge field. Hence the wire emulates a matter-coupled gauge theory, with fermion parity playing the role of the gauged global symmetry. Quantum phase slips lift the ground state degeneracy associated with unpaired Majorana edge modes at the ends of the chain, a change that can be understood as a transition between the confined and the Higgs-mechanism regimes of the gauge theory. We identify the quantization of thermal conductance at the transition as a robust experimental feature separating the two regimes. We explain this result by establishing a relation between thermal conductance and the Fredenhagen-Marcu string order-parameter for confinement in gauge theories.

